

Reproducibility of Regional Climate in Central Japan Using the 4-km Resolution WRF Model

Hiroyuki Kusaka¹, Tomoyuki Takata² and Yuya Takane²

¹*Center for Computational Sciences, University of Tsukuba, Tsukuba, Japan*

²*Graduate School of Life and Environmental Sciences, University of Tsukuba, Tsukuba, Japan*

Abstract

The present study provides a preliminary evaluation of the WRF model at 4-km horizontal resolution in central Japan with a 5-year control simulation. The results show that the spatial distribution of the annual mean temperature is well reproduced with a bias of +0.6°C. However, the diurnal range is underestimated by 1.8°C, which is mainly caused by an overestimation of the daily minimum temperature from October to April. Additional analyses indicate that there is a statistically significant correlation between the monthly bias and the number of clear sky days in a particular month, which implies the incomplete reproduction of the surface inversion layer at night. The model overestimates the annual precipitation amount averaged over the analysis domain by 7%, compared to the observations. Such a positive bias results from the overestimation of weak precipitation. On the other hand, the model underestimates the frequency of the heavy rainfall. The performance of the WRF model shown in this study is similar to that of the NHRCM (by Sasaki et al. 2008). The results indicate that the WRF model can be used for high resolution, regional climate simulation/projection research for the studied region.

1. Introduction

Regional Climate Models (RCMs) have been contributing to numerical simulations and projections of regional climate since Dickinson et al. (1989), Giorgi and Bates (1989), and Kida et al. (1991). Early studies used RCMs with a horizontal resolution of one hundred kilometers. Thereafter, due to the progress of super computers and RCMs, the spatial resolution of RCMs increased (e.g., Wang et al. 2004). In the early 2000s, the inter-comparison study of RCMs with 60-km horizontal resolution was performed (e.g., Takayabu et al. 2007).

Currently, RCMs are mainly used for high-resolution, regional climate simulation/projection (e.g., Sasaki et al. 2008; Kanada et al. 2008). The Weather Research and Forecasting (WRF) model (Skamarock et al. 2008; Kusaka 2009), is one of the RCMs used in big projects, such as the S-5 in Japan. Applying the WRF model to the Japanese weather and climate system is not yet satisfied, although the number of users has been increasing since Kusaka et al. (2005a, b). Recently, Hara et al. (2008) conducted a present climate simulation and future climate projection using the WRF model with 5-km horizontal resolution. However, it was only for a one month simulation.

As far as we know, there have been no reports on the multi-year regional climate simulations by the WRF model with horizontal grid spacing less than 5-km so far (Dudhia 2010; personal communication). Considering the research situation and the increasing number of WRF users, it is important to evaluate the performance of the WRF model for high resolution, regional climate simulations.

The purpose of the present study is to evaluate the performance of the WRF model with 4-km horizontal resolution for a

5-year control simulation. Furthermore, an indirect comparison with the NHRCM (Non-Hydrostatic Regional Climate Model, developed by the JMA/MRI) evaluated in a previous study (Sasaki et al. 2008) will be described. A comparison with the NHM (Non-Hydrostatic NWP Model, developed by the JMA/MRI) was previously performed by Hayashi et al. (2008). However, the target was very different from the present study (simulation period of one month and horizontal resolution of 20 km in Hayashi et al. 2008). Comparisons between the two major models can help to identify what produces the differences between the simulation and observations. Additionally, the comparison can also help to determine the uncertainties of RCMs, which will be beneficial to model developers and users.

2. Design of numerical simulation

The model domain (Fig. 1), which covers central Japan, is slightly different from Sasaki et al. (2008) because the present simulation does not use the nesting method (Sasaki et al. 2008, uses 10 km/4 km nesting). Horizontal grid spacing is set at 4 km. The model top is set to be 50 hPa, and 31 vertical sigma levels are used. Time integration is continuously conducted from August 1, 2001 to September 31, 2006. The first month was considered as the model spin-up. The initial and boundary conditions are created from the JMA-RANAL data (atmosphere), NCEP-FNL data (land surface), and the NCEP-RTGSST data (sea surface). The following schemes are used in the simulation in accordance with Hayashi et al. (2008): the Dudhia simple short wave radiation scheme, RRTM long wave radiation scheme, WSM3 cloud microphysics, Noah land surface model, and YSU atmospheric boundary layer scheme; no cumulus parameterization is used. Descriptions of these schemes, as well as references, are provided in Skamarock et al. (2008). Land use and terrain height data set created by the Geospatial Information Authority of Japan is used in the present study.

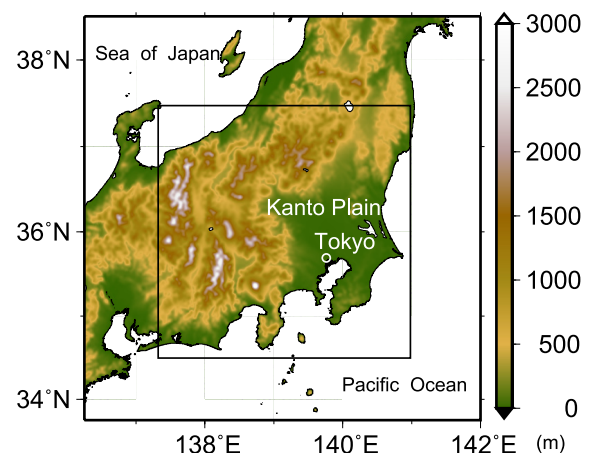


Fig. 1. Topography of the domain used in the numerical simulation. The inner solid line indicates the analysis domain, which is the same as Sasaki et al. (2008).

3. Results

3.1 Surface air temperature

The present study first evaluates the representation of surface air temperature from the WRF model simulation against the observations from the Automated Meteorological Data Acquisition System (AMeDAS) network. Here, the model temperature is modified with the temperature lapse rate of $0.0065^{\circ}\text{C m}^{-1}$ to consider the difference in the terrain height between the model grid and observation site. Figure 2 shows the horizontal distributions of annual mean surface air temperature from observation, simulation, and the difference between the observation and simulation. The horizontal distribution of the simulated temperature is roughly in agreement with that of the observation. Annual mean bias averaged over the plains and mountains is $+0.8^{\circ}\text{C}$ and $+0.3^{\circ}\text{C}$, respectively (Fig. 3). Annual mean bias averaged over the analysis domain is $+0.6^{\circ}\text{C}$ as the positive bias of the daily minimum temperature and negative bias of the daily maximum temperature are partially offset (the annual mean bias of the minimum and maximum temperatures are $+1.2^{\circ}\text{C}$ and -0.5°C , respectively). This is comparable to that of the NHRCM with $+0.8^{\circ}\text{C}$ (Sasaki et al. 2008). On the other hand, the diurnal range averaged over the analysis domain during the simulation period is underestimated by 1.8°C . Such a tendency is clearly seen from autumn to winter. The seasonality of the bias shows slight differences from that of the

NHRCM.

3.2 Precipitation

Figure 4 shows the horizontal distribution of annual precipitation from the observation (AMeDAS data), simulation, and ratio of the simulation against observation. The bias of the analysis domain is 7% (Fig. 5), which is similar to that of the NHRCM. Generally, the precipitation pattern is well reproduced in the plain and the spatially averaged bias of the plain is 3%, although the model overestimates precipitation in the northern part of the Kanto plain, and underestimates in the coastal areas. The spatial pattern of the bias is roughly in agreement with that of the NHRCM (Fig. S2, Supplement 1) except for the coastal areas of the Pacific Ocean.

Seasonal variation of the total precipitation amount over the analysis domain is illustrated in Fig. 6a. The model reproduces the seasonal variation well, although overestimation is seen in January, May, November and underestimation in July. The positive bias in May and negative bias in July are also found in the NHRCM (Fig. S3, Supplement 2). Figure 6b shows the frequency of precipitation intensity calculated from three-hourly accumulated precipitation amount. Overall, the model simulation is in good agreement with the observations. However, the frequency of heavy precipitation is underestimated in the model. Such a tendency is not found in the NHRCM (Fig. S4, Supplement 2).

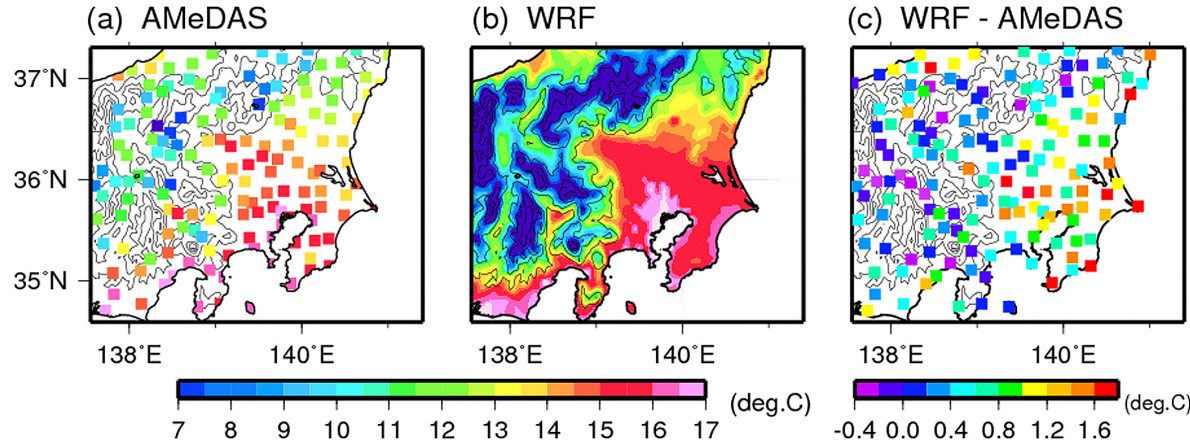


Fig. 2. Spatial distribution of surface air temperature averaged for 5-years. (a) Observation, (b) simulation, (c) the difference between the observation and the simulation (simulation minus observation).

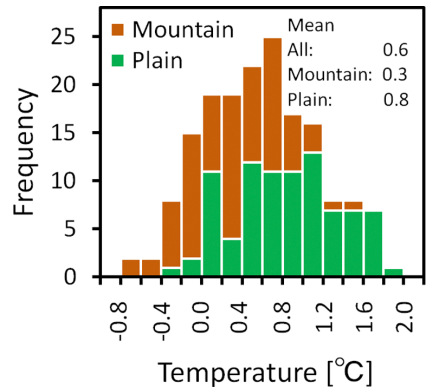


Fig. 3. Frequency (individual observation sites) of the temperature difference between the simulation and observation at the observation sites within the analysis domain. The temperature is averaged for 5-years.

Table 1. Bias of the monthly averaged daily mean, maximum, and minimum temperatures.

	WRFmean	Diffmean	Diffmax	Diffmin	Diffrange
JAN	1.8	0.5	-0.8	1.6	-2.4
FEB	3.0	0.4	-0.9	1.4	-2.3
MAR	6.0	0.6	-0.9	1.5	-2.4
APR	12.4	0.9	-0.6	1.8	-2.5
MAY	16.0	0.2	-1.0	0.7	-1.7
JUN	20.4	0.2	-0.6	0.5	-1.0
JUL	23.7	0.4	-0.2	0.5	-0.7
AUG	24.8	0.3	-0.6	0.6	-1.2
SEP	21.6	0.6	-0.1	0.9	-1.0
OCT	15.7	1.0	-0.1	1.6	-1.7
NOV	10.3	1.2	-0.3	2.2	-2.4
DEC	4.2	0.8	-0.5	1.7	-2.2
Mean	13.3	0.6	-0.5	1.2	-1.8

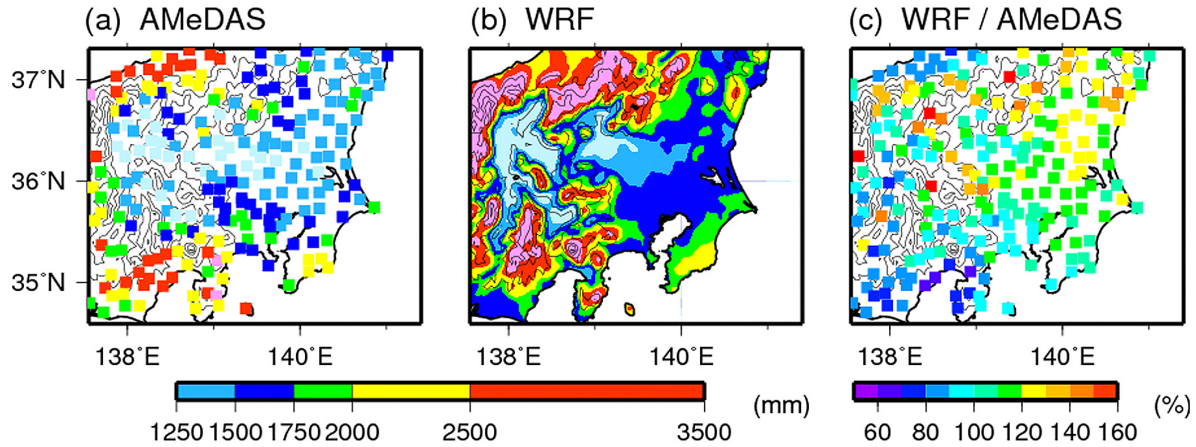


Fig. 4. Accumulated precipitation amount during the 5-year period. (a) Observation, (b) simulation, (c) the ratio between the simulation and observation (simulation/observation).

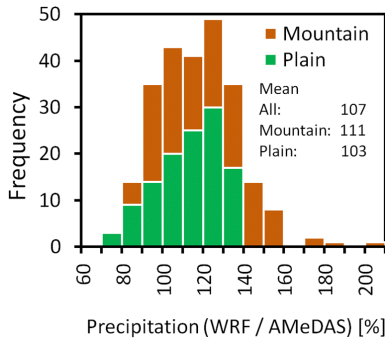


Fig. 5. Frequency (individual observation sites) of the ratio between the simulation and observation.

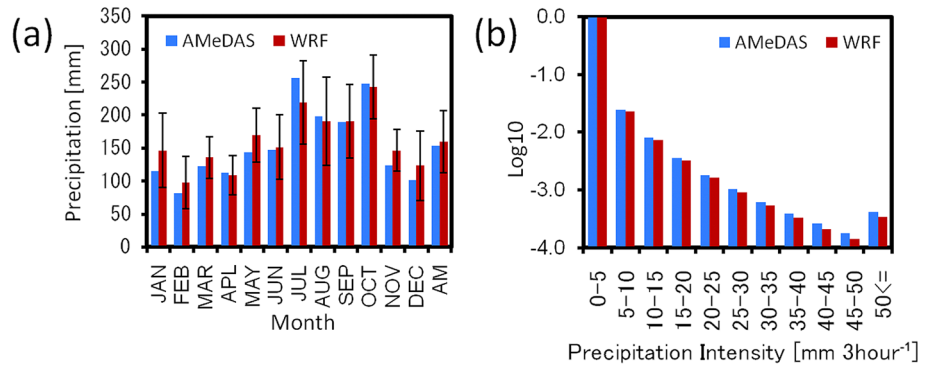


Fig. 6. (a) Monthly and annual mean precipitation spatially averaged over the analysis domain. The annual mean (AM) precipitation is divided by 12. The red and blue vertical bars indicate the simulation and observation, respectively. The error bars present the standard deviation of the difference between the simulation and observation in space. (b) Frequency of precipitation intensity per three hours. The frequency is normalized by total number and shown by logarithm indication.

4. Discussion

Analyses in the previous section show that the diurnal surface air temperature range from the model is underestimated by 1.8°C , which is mainly caused by the overestimation of the daily minimum temperature from October to April. Figure 7a shows a scatter diagram of the number of clear sky days (daily sunshine duration is more than 6 hours without precipitation) versus the bias of daily minimum temperature averaged at the observation sites in the analysis domain. According to the diagram, the bias becomes larger as the number of clear sky days increases. Such a relationship is especially prominent in April and November with large bias. The correlation coefficient is 0.61, which is statistically significant at the 1% level. Additionally, the relationship between sunshine duration and bias in April 2004 (positive temperature bias of more than 1.5 standard deviations) is consistent with the above findings, as illustrated in Fig. 7b. The results imply the incomplete reproduction of the strong nocturnal inversion layer in the model due to the coarse vertical grid spacing near the surface in the model, i.e., the lowest grid point is about 30 m above the ground level, overestimating the vertical diffusion coefficient under stable conditions, and/or due to the overly strong effect of the vegetation canopy.

As described in the previous section, the annual precipitation amount averaged over the analysis domain is overestimated by 7% compared to the observations. Figure 8 classifies the annual

precipitation from the simulation and observation, categorized by the observed precipitation intensity. It is found that such a positive bias results from the overestimation of weak precipitation. On the other hand, the model tends to underestimate the frequency of the heavy rainfall, which is not seen in the NHRCM. These are probably caused by a systematic bias of the model, perhaps from the WSM3 cloud microphysics scheme without graupel (Fig. S6, Supplement 4).

5. Summary

The present study provides a preliminary evaluation of the WRF model at 4-km horizontal resolution in central Japan with a 5-year control simulation. Simulated results are summarized as follows.

- (1) The spatial distribution of the annual mean temperature is reproduced well. The bias averaged over the analysis domain is $+0.6^{\circ}\text{C}$, which is comparable to that of the NHRCM (by Sasaki et al. 2008). However, the spatial distribution of the bias is different from the NHRCM.
- (2) The diurnal range averaged over the analysis domain is underestimated by 1.8°C , which is mainly caused by the overestimation of the daily minimum temperature from October to April. Additional analyses indicate that there is a statistically significant correlation between the bias and the number of clear sky days, which implies the incomplete reproduction of

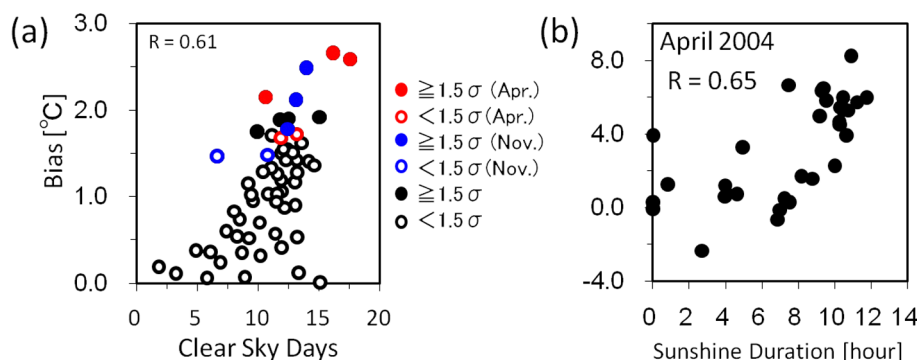


Fig. 7. (a) Scatter diagram of the number of clear sky days versus bias of the daily minimum temperature for each month. All circles indicate individual months, red circles indicate April and blue circles indicate November. Solid circles indicate months with a large bias of more than 1.5 sigma level. All data are monthly mean values and averaged over the analysis domain. (b) Scatter diagram of daily sunshine duration versus bias of the daily minimum temperature in April 2004. All data are averaged over the analysis domain.

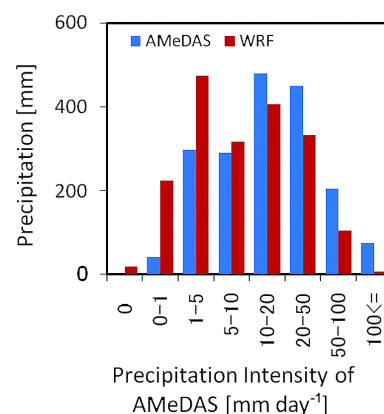


Fig. 8. Accumulated daily precipitation for the 5-year period, categorized by the intensity of observed precipitation.

the strong surface inversion layer at night.

- (3) The model overestimates the annual precipitation amount averaged over the analysis domain by 7%, compared to the observations. Such a positive bias results from the overestimation of weak precipitation.
- (4) The frequency of heavy precipitation is underestimated, which is not consistent with the results from the NHRCM.

The performance of the WRF model is similar to that of the NHRCM. The results indicate that the WRF model can be used for high resolution, regional climate simulation/production research for the studied region. For larger regions, the spectral or grid nudging can be needed. The evaluation of the WRF model for larger regions would be a potential subject for future studies.

Acknowledgments

This study was supported by the Global Environment Research Fund (S-5-3) of the Ministry of the Environment, Japan. Numerical simulations for the present work have been carried out under the “Interdisciplinary Computational Science Program” in the Center for Computational Sciences, University of Tsukuba.

Supplements

The same type of the figures as Fig. 2c and Fig. 4c from Sasaki et al. (2008) are shown in Supplement 1. The same type of figure as Fig. 6 from Sasaki et al. (2008) is shown in Supplement 2. Time series of the daily maximum and minimum temperatures is illustrated in Supplement 3. Result from the model inter-comparison between cloud microphysics schemes is shown in Supplement 4.

References

- Dickinson, R. E., R. M. Errico, F. Giorgi, and G. T. Bates, 1989: A regional climate model for the western U. S. *Clim. Change*, **15**, 383–422.
- Giorgi, F., and T. Bates, 1989: The climatological skill of a regional model over complex terrain. *Mon. Wea. Rev.*, **117**, 2325–2347.
- Hara, M., T. Yoshikane, H. Kawase, and F. Kimura, 2008: Estima-

tion of the impact of global warming on snow depth in Japan by the pseudo-global-warming method. *Hydrol. Res. Lett.*, **2**, 61–64.

- Hayashi, S., K. Aranami, and K. Saito, 2008: Statistical verification of short term NWP by NHM and WRF-ARW with 20 km horizontal resolution around Japan and Southeast Asia. *SOLA*, **4**, 133–136.
- Kanada, S., M. Nakano, S. Hayashi, T. Kato, M. Nakamura, K. Kurihara, and A. Kitoh, 2008: Reproducibility of maximum daily precipitation amount over Japan by a high-resolution non-hydrostatic Model. *SOLA*, **4**, 104–108.
- Kida, H., T. Koide, H. Sasaki, and M. Chiba, 1991: A new approach to coupling a limited area model with a GCM for regional climate simulations. *J. Meteor. Soc. Japan*, **69**, 723–728.
- Kusaka, H., 2009: About a regional atmospheric model WRF. *Nagare*, **28**, 3–12, (in Japanese).
- Kusaka, H., A. Crook, J. Knierel, and J. Dudhia, 2005a: Sensitivity of the WRF model to advection and diffusion schemes for simulation of heavy rainfall along the Baiu front. *SOLA*, **1**, 177–180.
- Kusaka, H., A. Crook, J. Knierel, J. Dudhia, and K. Wada, 2005b: Comparison of the WRF and MM5 models for simulation of heavy rainfall along the Baiu front. *SOLA*, **1**, 197–200.
- Sasaki, H., K. Kurihara, I. Takayabu, and T. Uchiyama, 2008: Preliminary experiments of reproducing the present climate using the non-hydrostatic regional climate model. *SOLA*, **4**, 25–28.
- Skamarock, W. C., J. B. Klemp, J. Dudhia, D. O. Gill, D. M. Barker, M. G. Duda, X.-Y. Huang, W. Wang, and J. G. Powers, 2008: A description of the advanced research WRF version 3. *NCAR/TN-475+STR*, 113 pp.
- Takayabu, I., H. Kato, K. Nishizawa, Y. N. Takayabu, Y. Sato, H. Sasaki, K. Kurihara, and A. Kitoh, 2007: Future projections in precipitation over Asia simulated by two RCMs nested into MRI-CGCM2.2. *J. Meteor. Soc. Japan*, **85**, 511–519.
- Wang, Y., L. R. Leung, J. L. McGregor, D.-K. Lee, W. C. Wang, Y. Ding, and F. Kimura, 2004: Regional climate modeling: Progress, Challenges, and Prospects. *J. Meteor. Soc. Japan*, **82**, 1599–1628.

Manuscript received 11 June 2010, accepted 16 August 2010
 SOLA: <http://www.jstage.jst.go.jp/browse/sola/>